Investigation of magnetic wall shunt combinations on 650 MVA power transformers by finite element methods

ABSTRACT

Power transformer losses mainly include open circuit loss and short circuit loss. Open circuit loss is created in the iron core of the transformer. Short circuit loss, copper loss, and stray loss are known collectively as “short circuit loss”. Copper loss is created in windings: current flows through the DC resistance in windings. Stray loss is caused by eddy currents in high magnetic permeability and high conductivity of components such as tanks, windings, and structural parts. This is why the volume limit of power transformers and the ratio of stray loss in structural parts and the tank cannot be ignored. This has led transformer manufacturers to add magnetic wall shunts to reduce stray loss. But often, too many magnetic wall shunts are added or misplaced, which results in increased cost and reduced performance. By improving stray loss distribution in power transformers, magnetic wall shunt design can be optimized, and the tradeoff of cost and performance can be balanced.

KEYWORDS:

Stray loss, Magnetic wall shunts, Finite Element Methods (FEM), Eddy current, Thermal analysis

Technical specifications, manufacturing costs, capitalization costs, and material costs must be considered to optimize transformer design

Controlling stray loss, and the resulting hot spots and temperature rises can be the most important way to ensure the proper operation of a transformer

1 Introduction

Today, transformer design has been limited by size due to field applications and transportation. As such, power transformer designers account for efficiency, insulation, and cooling systems. Technical specifications, manufacturing costs, capitalization costs, and material costs must be considered to optimize transformer design. [1] Therefore, stray loss in metal parts cannot be ignored as the capacities of power transformers increase. [2] This has led transformer manufacturers to add magnetic wall shunts to reduce stray loss. However, when too many magnetic wall shunts are added or misplaced, transformer cost increases and performance decreases. Therefore, the stray loss distribution of power transformers should be investigated. The optimal design of magnetic wall shunts can be balanced against cost and performance. [3] Present-day transformer manufacturers should use Finite Element Methods (FEM) to analyze power transformers. Design can be optimized when transformer operating conditions are predicted accurately. [4]

In this study, ANSYS@Maxwell and ANSYS@Mechanical modules were used to optimize the application of magnetic wall shunts and decrease the temperature rise in magnetic components of a transformer [5].

The literature includes research which determines and reduces hot spots on tank walls and other structural components of a transformer. To determine hot spots, transformer stray loss should be examined. Calculation of stray loss is not a simple task; the transformer has a nonuniform structure. The calculation is complex because of the following:

- modeling of magnetic nonlinearity,
- difficulty in calculating stray areas and effects quickly and accurately,
- inability to isolate certain stray loss components from the load under test,
- limitations of experimental verification methods for large power transformers.

Multiple studies are conducted here to reduce transformer losses, and the best selected. A thermal model is proposed as a result of the latter in order to obtain temperature distribution in a transformer. The proposed model is formulated with ANSYS@Maxwell and ANSYS@Mechanical software, which performed field analyses and solved energy equations based on FEM. These values are calculated using transformer characteristics and dimensions. Losses generated heat in the thermal analysis procedure. The expected results were to find the hottest region in a transformer by determining the temperature distribution in its basic components. Finally, the thermal field of a 650MVA oil-immersed autotransformer was modeled in 3D and analyzed by FEM.

2 Design parameters

Transformer design parameters are shown in Table 1. The voltage and number of turns used in the analyses are also given in the table. Three different cooling stages are included, depending on the rated power.

Controlling stray loss, and the resulting hot spots and temperature rises can be the most important way to ensure the proper operation of a transformer. Eddy current loss is a large portion of the stray loss. Magnetic leakage and eddy current loss must be examined in depth. [6-7] A 3D geometric model of the power transformer is created and analyzed with FEM 3D. Different types of magnetic wall shunts are used to reduce eddy current loss in the transformer. The effects of wall shunts on eddy current loss are discussed below.

Table 1. Design Parameters of the Autotransformer

Rated power	650 MVA			
Connection type	YNa0d11			
Cooling system	ONAN / ONAF I / ONAF II			
Core leg type	3 / 0			
Frequency (Hz)	50			
Core material	MOH-0.75			
	HV Winding	LV Winding	LV – TAP Winding	TV Winding
Rated voltage (kV)	420	170	170	46
Number of turns	468	368	78	131
Current (A)	938.2	981.4	981.4	1514.6

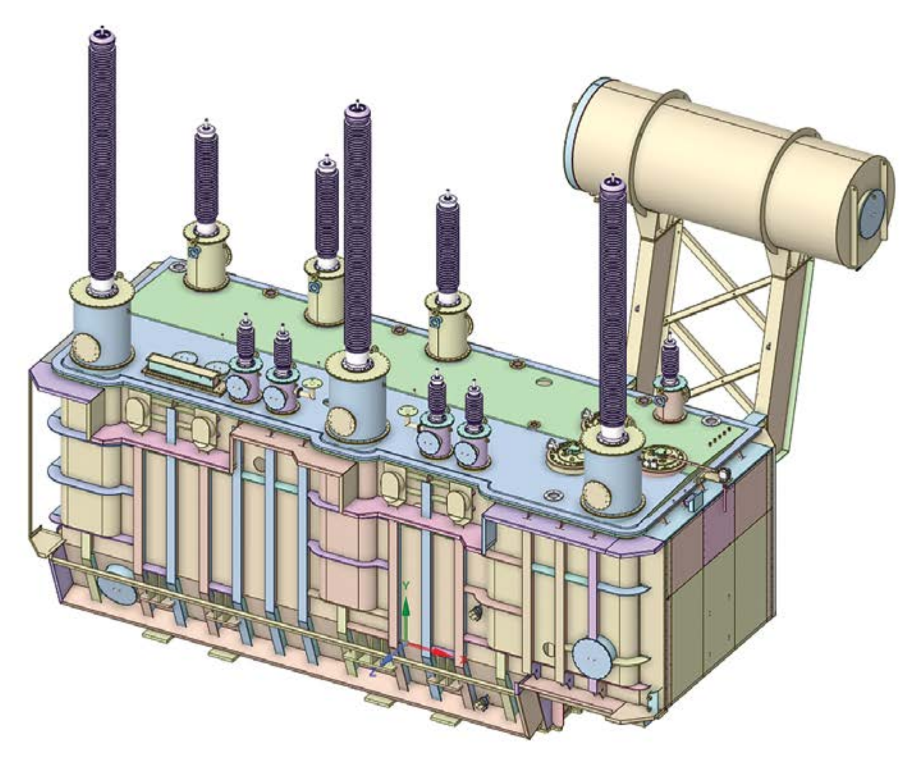

Figure 1. 650 MVA Autotransformer Model

3 Theory

3.1. Stray Loss

Leakage flux causes eddy currents in transformer windings, which generates heat. This power loss is called "stray loss." Stray loss in the transformer tank can be estimated by means of the Poynting vector. Maxwell's equations are used to calculate stray loss. [8-10]

Stray loss in tank walls and yoke beams is calculated using surface impedance boundary conditions. Magnetic wall shunts are modeled with nonlinear anisotropic permeability; corresponding losses are calculated by FEM. [8-10]

$$\nabla x\mathbf{E} = -\frac{\partial \mathbf{B}}{\partial t}$$

$$\nabla x\mathbf{H} = \mathbf{J}$$

$$\nabla.\mathbf{B} = 0$$

Where:

H = magnetic field strength (A/m)
E = electric field strength (V/m)
B = flux density (T)
J = current density (A/m^2)
D = electric flux density (C/m^2)

Two constitutive equations are:

$\mathbf{J} = \sigma\mathbf{E}$
$\mathbf{B} = \mu\mathbf{H}$

Where:

μ = permeability of material (H/m)
σ = conductivity of material (S/m)

$$\nabla(\nabla.H) - \nabla^2 H = \nabla xJ$$

$$\nabla^2 H - \mu\sigma\frac{\partial H}{\partial t} = 0$$

Assume a structural component (see Figure 2). Magnetic field intensity H_y and current density J_x are functions of z. Complex permeability can be written in the equation for this problem.

$$\frac{d^2H_y}{dz^2} = j\omega\sigma\mu H_y$$

$$\text{At } z = 0,\ H_y = H_a e^{-mz}$$

$$m = \sqrt{j\omega\sigma\mu} = (1+j)\sqrt{\frac{\omega\sigma\mu}{2}}$$

Where H_a is a constant and m is the propagation constant.

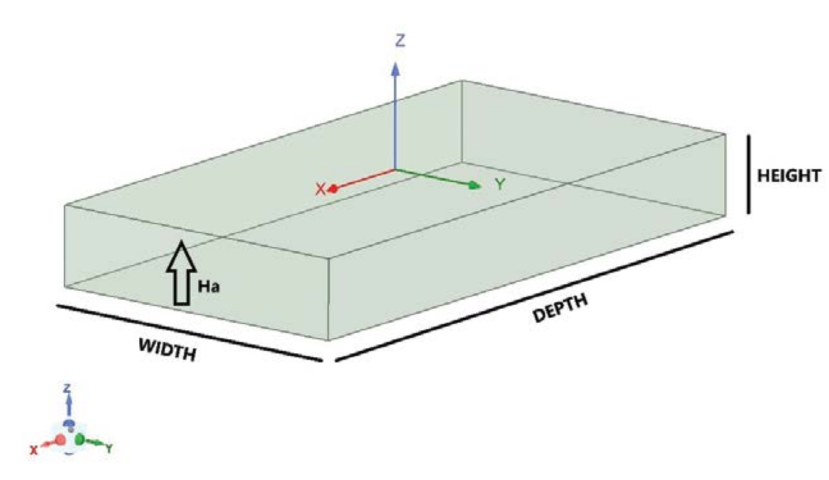

Figure 2. Stray Loss in Structural Components

> **Leakage flux causes eddy currents in transformer windings, which generates heat, and the corresponding power loss is called "stray loss"**

$$H_y = H_a e^{\frac{-(1+j)z}{\delta}}$$

Simplifying by putting equations in place, the following emerges.

$$J_x = \frac{(1+j)}{\delta} H_a e^{\frac{-(1+j)z}{\delta}}$$

Calculating the real part of the complex Poynting vector at the surface gives the time-averaged density of stray loss from the transformer tank.

$$P = \frac{1}{2} R[ExH]$$

On the surface (z = 0), the stray loss per unit surface area is

$$P = \sqrt{\frac{\mu\omega}{8\sigma}} \int_{surface}^{\square} H_a^2 d_s$$

> **Coupled electromagnetic and thermal finite element calculations should be conducted to estimate the stray losses and the hot spots**

3.2. Thermal

Radiation

For the outer surface, heat radiation is expressed in the equation below:

$$q''(z) = \frac{q}{A} = \varepsilon\sigma(T_s^4 - T_{air}^4)$$

where q is the local radiation heat, transferred in height z in the outer surface (W), q" is the local radiation heat flux in height z in the outer surface (W/m^2), h the local heat transfer coefficient for radiation from the outer surface (W/(m^2 °C)), ε the emissivity coefficient of the surface, T_s the local temperature of the surface (°C), T_{air} the air temperature (°C), A the surface on which radiation occurs (m^2), and r is Stefan-Boltzmann's coefficient (5.67 X $10^{(-8)}$ W/(m^2, K^4)).

Natural Convection

$$q''(z) = \frac{q}{A} h(T_s - T_{air})$$

$$h(z) = \frac{Nu_z k_{air}}{Z}$$

$$Nu_z = \left[\frac{4Pr^2 Gr^*}{36 + 45Pr}\right]^{\frac{1}{5}}$$

$$Gr^* = \frac{g\beta q'' z^4}{k_{air}\vartheta^4}$$

where q is the local convection heat, transferred in height z in the outer surface (watt), q the local convection heat flux at location z in the outer surface (W/m^2), q" co the average heat flux in the outer surface (W/m^2, h the local heat transfer coefficient for convection from the outer surface (W/(m^2 °C), k_{air} the thermal conductivity of air °C), Gr^* the Grashof number for uniform heat flux, Nuz the Nusselt number, Pr the Prandtl number, β the volumetric expansion of air (1/°C), ν the kinematical viscosity of air (m | 2⁄s), g the acceleration of gravity (m/s^2), and z is the vertical distance (m). The above mentioned equations are valid over Grashof's range ($10^5 \leq Gr^* \leq 10^{10}$). [11-12] Note that β, ν, and k_{air} are dependent on unknown temperatures. [13]

Conduction

$$Q = kA\nabla T$$

Conduction heat is transferred from the hotter end to the colder end of a material. The ability of the material to conduct heat is known as thermal conductivity and is denoted k (W/mK). Variable "A" is the surface conduction transfer area. ΔT is differential tempera-

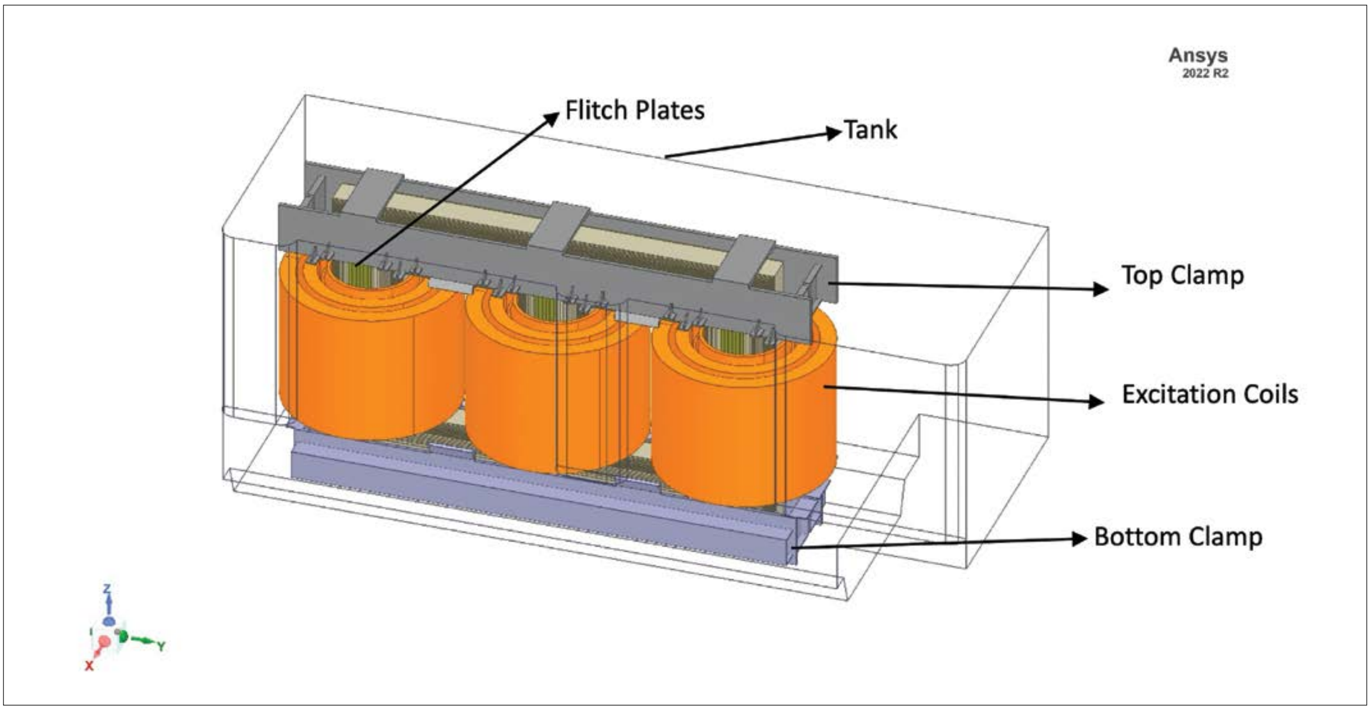

Figure 3. 3D Analysis Model of an Autotransformer

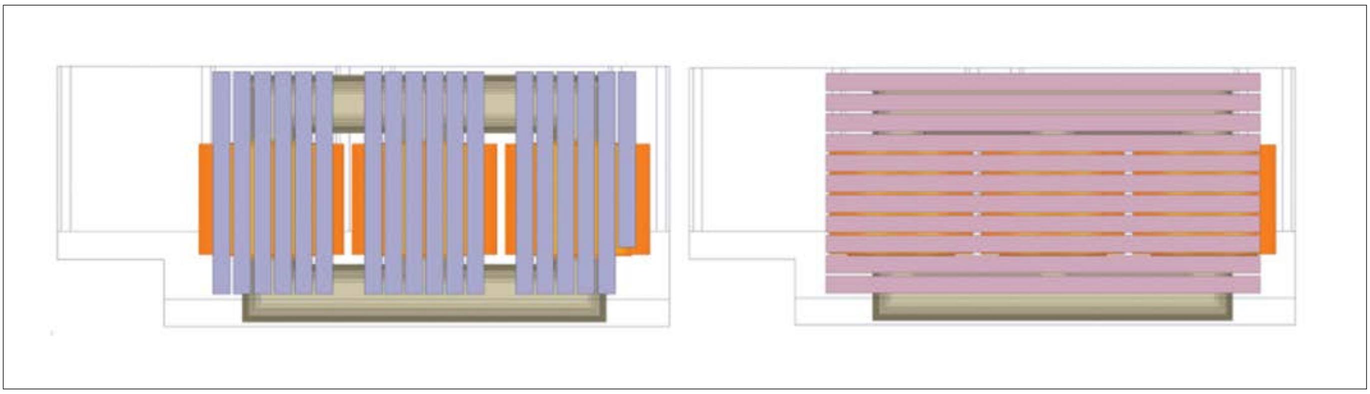

Figure 4. Different Combinations of Tank Wall Shunts

> **Two different wall shunt combinations are modeled for an autotransformer: one with 18, 35mm thick, magnetic wall shunts placed vertically, and the other with 11, 21 mm thick wall shunts placed horizontally on LV side walls**

ture between a cold surface and a hot surface.

4. Finite element analysis model

4.1. Autotransformer Simulation Model

The 3D model of a three-phase, three-limb transformer is shown in Figure 3. The model is composed of the excitation coil, iron core, and test environment.

Two different wall shunt combinations are modeled for an autotransformer. In one, 18 magnetic wall shunts, 35 mm thick were placed vertically on LV walls of the transformer tank. In the other, 11 wall shunts, 21 mm thick, were placed horizontally on LV walls.

4.2 Electromagnetic Analysis

Eddy current fields and the losses in the structure parts of the transformer are analyzed, as well as eddy current loss distributions in tank walls and clamps.

Capacity is 650 MVA, the rated voltage of the HV side is 420 kV, and the rated voltage of the LV side is 170 kV. The voltage adjustment range is about 10% on the LV side: the maximum voltage is 187 kV, and the minimum 153 kV.

Transformers have an active part and a whole tank with base geometry for modeling. The core, its clamping structure (frames and Flitch Plates), windings, transformer tank, and wall shunts are constructed as base components in the electromagnetic model.

The magnetic properties of materials are shown in Table 2. Relative permeability is defined in "B-H Curves" for more accurate results. The material type for tank walls and core frames (St-37-2) steel plate is "mild steel". The core's CRGO electrical steel is "MOH – 0.75". However, the wall shunts' CRGO electrical steel is M5, 0.50 mm wide. Stacking factors for "MOH – 0.75" and "M5" electrical steel are defined for stacking directions (X, Y, Z).

Peak current values, number of turns, and phase angles are used, respectively, as input data for each of the 3 wound phase legs in electromagnetic models, as shown in Table 3. Peak current values are given because of software conventions. Phase angles are provided because phases are 120 degrees apart.

> **Eddy current fields and the losses in the structure parts of the transformer are analyzed, as well as eddy current loss distributions in tank walls and clamps**

Table 2. Materials in the Simulation Model

Name	Material
Excitation Coil	Copper
Core	MOH-0.75
Clamps	Stainless Stell
Flitch Plates	St-37-2
Copper	St-37-2

Table 3. Excitation in the Simulation Model

Winding Name	Type	Phase	Excitation
HV-A	Current	0	938.2*468*√2
LV-A	Current	0	981.4*368*√2
TAP-A	Current	0	981.4*78*√2
HV-B	Current	120	938.2*468*√2
LV-B	Current	120	981.4*368*√2
TAP-B	Current	120	981.4*78*√2
HV-C	Current	240	938.2*468*√2
LV-C	Current	240	981.4*368*√2
TAP-C	Current	240	981.4*78*√2

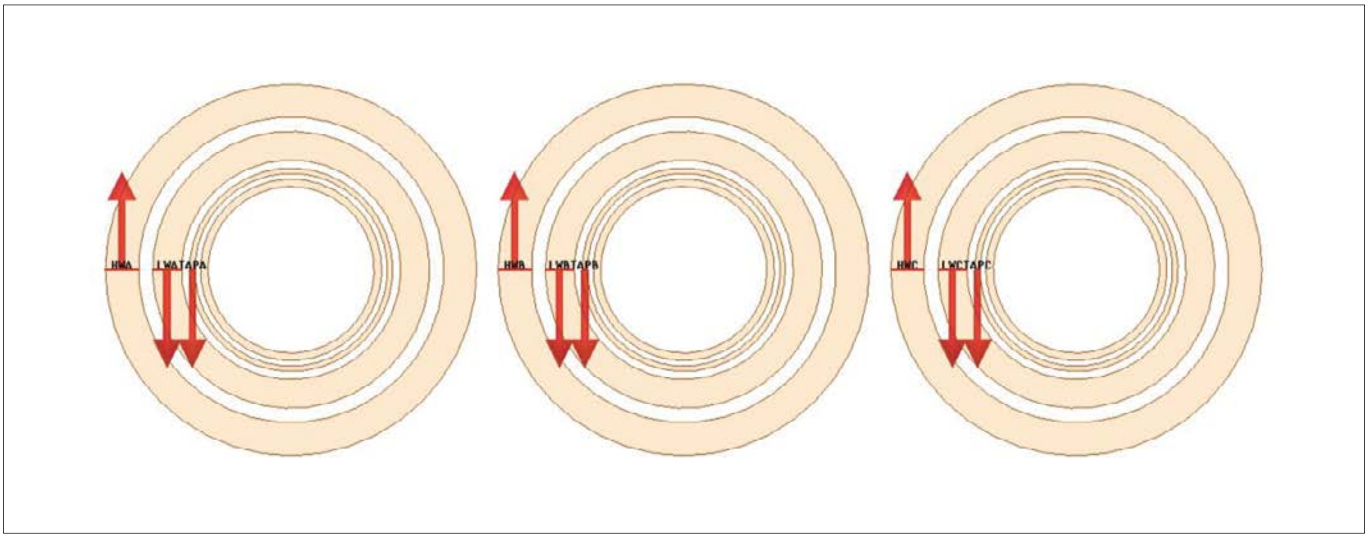

Figure 5. Winding Excitation and Direction

Temperature rises in transformer tank and steel are calculated with losses obtained from electromagnetic analyses

4.3. Thermal Analysis

Temperature rises in transformer tank and steel are calculated with losses obtained from electromagnetic analyses. Ambient temperature is defined on the outer surfaces of the transformer tank. Oil temperatures are defined at the inner surfaces of the tank and other metallic clamping parts' surfaces. Oil temperature is defined as a gradient from bottom to top. Ambient temperatures and bottom and top oil temperatures are determined by formulae in IEC 60076 and in design tools created by the BEST transformer company.

In thermal analyses, heat radiation is defined at the outer surface of the tank, which demonstrates the efficacy of thermal radiation cooling. Emissivity is taken from RAL paint tables. Convection from the tank to air is also defined at the outer surface of the tank. The convection coefficient of air is taken directly from the ANSYS Mechanical Library. On the other hand, convection boundary conditions for oil are defined at the inner surfaces of the tank and the other metallic parts. Convection coefficients are obtained and validated by internal studies as well as tests performed for BEST transformers. Convection coefficients are shown in Figure 6.

Stray loss and temperature distribution in three-phase, three-limb power transformers are analyzed by simulation and FEA modeling

5. Finite Element Analysis Results

Stray loss and temperature distribution in three-phase, three-limb power transformers are analyzed by simulation and FEA modeling. First, stray and maximum total losses are analyzed by 3D FEA models. Next, stray losses from ANSYS MAXWELL are defined as inputs to ANSYS MECHANICAL. Accordingly, the temperature distribution in an autotransformer is examined for metal parts (clamps, Flitch Plates).

The 3D FEM analysis reveals that horizontal magnetic wall shunt combinations prevail thermally and volumetrically.

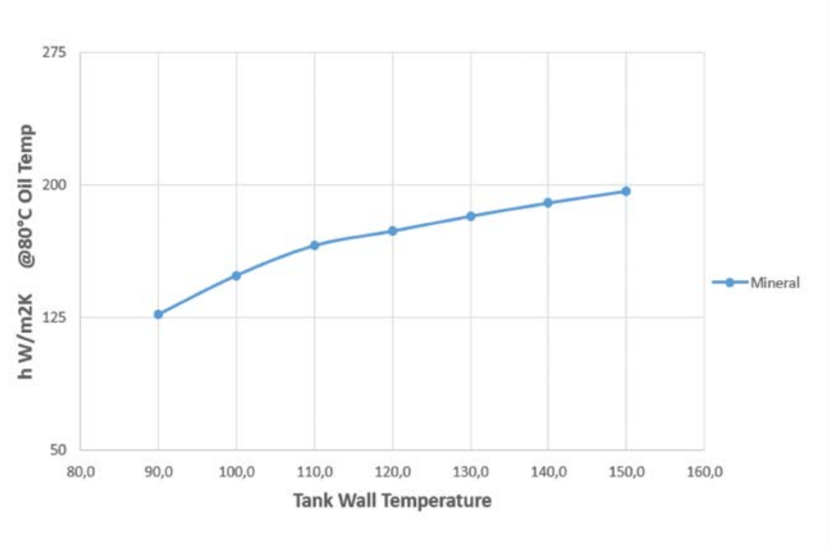

Figure 6. Convection Coefficient vs. Temperature

6. Conclusion

Effects of horizontal and vertical wall shunt arrangements are examined. Reductions of leakage loss in power transformers are compared. The investigation is carried out by 3D FEA using ANSYS@ Maxwell and ANSYS@Mechanical. The efficacy of magnetic wall shunt orientation for autotransformers is evaluated by means of 3D FEM. The problem was solved as a nonlinear, multi-objective, constrained optimization problem. The leading method is presented with several optimizations. The hot spot temperature was below temperature rise limits defined in IEC tables: no hazard is foreseen for insulation material with respect to temperature endurance limits. The 3D FEM analyses for this autotransformer demonstrate that horizontal magnetic wall shunts provide the best thermal and volumetric results due to collecting and cancelling three-phase leakage fluxes. However, horizontal shunts are not as effective as vertical shunts on end walls, where most leakage flux is single phase, without much cancellation. As such, the former reduces losses and temperatures less effectively. Finally, horizontal shunts are less effective on zero sequence flux caused by system events such as Ground Induced Currents (GIC) or unbalanced phase loads. Accordingly, practical transformer designs should continue to utilize vertical shunts.

Table 4. Results of Thermal Analyses

Combination	Hot spot (°C)				Shunts Volume (m³)
	Tank	Top Clamp	Bottom Clamp	Flitch Plate	
Vertical Magnetic Shunt (35mm)	111.30	122.92	122.30	112.31	7.2
Horizontal Magnetic Shunt (25mm)	104.6	122.17	122.03	112.2	6.2

Table 5. Temperature Distribution of an Autotransformer

Vertical Magnetic Shunt (35mm)	Horizontal Magnetic Shunt (25mm)
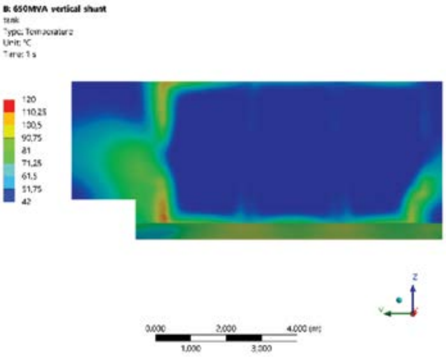	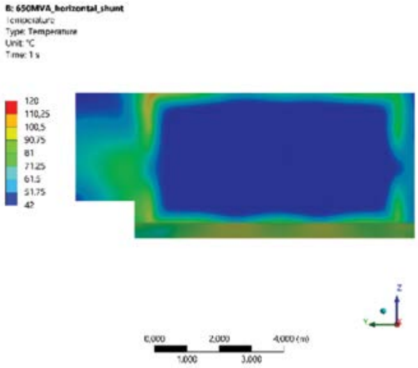

7. References

[1] W. C. Chang and C. C. Kuo, “A novel excitation approach for power transformer simulation based on finite element analysis,” Applied Sciences, vol. 11, no. 21, p. 10334, 2021.

[2] A. S. Reddy and M. Vijaykumar, “Hottest Spot and Life Evaluation Of Power Transformer Design Using Finite Element Method,” Journal Of Theoretical & Applied Information Technology, vol. 4, no. 3, 2008.

[3] M. A. Tsili, A. G. Kladas, P. S. Georgilakis, A. T. Souflaris, and D. G. Paparigas, “Geometry optimization of magnetic shunts in power transformers based on a particular hybrid finite-element boundary-element model and sensitivity analysis,” IEEE Transactions on Magnetics, vol. 41, no. 5, pp. 1776-1779, 2005.

[4] M. Moghaddami, A. I. Sarwat, and F. De Leon, “Reduction of stray loss in power transformers using horizontal magnetic wall shunts,” IEEE Transactions on Magnetics, vol. 53, no. 2, pp. 1, 2016.

[5] ANSYS Inc., “C.P.U.,” Available at: www.ansys.com, [Accessed: 1 June 2022].

[6] M. Rizzo, A. Savini, and J. Turowski, “Influence of flux collectors on stray losses in transformers,” IEEE Transactions on Magnetics, vol. 36, no. 4, pp. 1915-1918, 2000.

[7] M. V. Vega, R. E. Perez, and T. Niewierowicz, “3D finite element estimation of stray losses in three-phase transformers,” Journal of applied computer science, vol. 16, no. 1, pp. 89-100, 2008.

[8] S. V. Kulkarni and S. A. Khaparde, “Transformer engineering: design, technology, and diagnostics,” CRC press, 2017.

[9] J. U. Kothavade and P. Kundu, “Investigation of Stray Losses in Converter Transformer Using Parametric Analysis of Wall Shunt Thickness,” Journal of Operation and Automation in Power Engineering, vol. 11, no. 4, pp. 240-248, 2023.

[10] K. H. Park, H. J. Lee, and S. C. Hahn, “Finite-element modeling and experimental verification of stray-loss reduction in power transformer tank with wall shunt,” IEEE Transactions on Magnetics, vol. 55, no. 12, pp. 1-4, 2019.

[11] L. W. Pierce, “Predicting hottest spot temperatures in ventilated dry type transformer windings,” IEEE Transactions on Power Delivery, vol. 9, no. 2, pp. 1160-1172, 1994.

[12] T. L. Bergman, A. S. Lavine, F. P. Incropera, and D. P. DeWitt, “Introduction to heat transfer,” John Wiley & Sons, 2011.

[13] J. P. Holman, “Heat transfer,” McGraw Hill, 1986.

Authors

Ramazan Altay has been a researcher and R&D analysis division manager at BEST Transformer since 2021. He received a bachelor degree in machine engineering from Balıkesir university in 2012, a Masters degree in mechanical engineering from Balıkesir university in 2018, and has been enrolled at a doctorate program at the University of Cantbria since 2019. He started his career at BEST Transformer as a mechanical design engineer in 2014, becoming an R&D mechanical analysis engineer in 2017.

İrem Hazar has been a researcher and an R&D electrical analysis engineer at BEST Transformer since 2021. She received a bachelor degree in electrical and electronic engineering from the Celal Bayar University in Manisa in 2016, obtaining a Masters degree at the same university in 2020. Before her appointment at BEST, she worked at İşbir Elektrik Sanayi as an R&D engineer.

Necmettin Mert Koçanalı has been a researcher and an R&D mechanic analysis since 2021. He received a bachelor degree in machine engineering from the Katip Çelebi University in İzmir in 2021, and is currently working on obtaining a Masters degree in mechanical engineering at the same university.

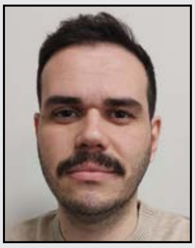

Caner Adışen has been a researcher and an R&D mechanic analysis since 2023. He received an undergraduate degree in machine engineering from the University of Balıkesir in 2012, and is currently working on obtaining a Masters degree in machine engineering at the same university.

Mahmut Aksoy has been the research and development manager at BEST Transformer since 2022. He graduated from the Istanbul Technical University in 2003 with a bachelor degree in Electrical Engineering. In 2012 he obtained an MBA at Istanbul Bilgi University. From 2008 to 2021, he was the director of electrical design and, from 2021-2022, the director of the development of design analysis in the company. Priorto his appointment at BEST, he worked in companies such as Vestel Beyaz Eşya A.Ş., Alarko-Carrier A.Ş. and Areva T&D.